

Isobaric Expansion Engines Powered by Low-Grade Heat—Working Fluid Performance and Selection Database for Power and Thermomechanical Refrigeration

Ahmad K. Sleiti

A database is developed for the most suitable working fluids for Worthington-type and Bush-type isobaric engines based on their performances for a wide range of heat source temperature, from 40 to 300 °C, and operating pressures from 1 to 100 bar. Thermodynamics models are developed and simulated to study the effects of different operating temperatures and pressures on the efficiency and back work ratio of both engines. Results show that in temperature range from 40 to 60 °C, the achieved efficiency is less than 4% for most cases, suggesting that practical applications in this range are very limited. Ammonia and R32 show the highest efficiencies ($\approx 11\%$) at high pressure of 50 bar for the temperature range of 100–300 °C. The refrigerant R161 has high performance for pressures between 10 and 50 bar for the full range of temperatures from 80 to 300 °C, which makes R161 the choice fluid for a wide range of applications. Novel applications are introduced, which integrate these isobaric engines with vapor compression refrigeration systems. The thermodynamic cycles of the heat driven compressor with the selected working fluids as in the current study and the simplified technological solutions are crucial components of the study novelty.

utilization and impose urgent calls for practical alternatives. One of those untapped alternatives is the potential of harnessing low-grade heat sources for cooling and refrigeration applications. Developing new integrated cooling/refrigeration systems that are able to work at low-grade heat temperatures with eco-friendly working fluids contributes meaningfully to the solution of these issues. Integration of energy systems for double,^[5] triple,^[6] and even quadruple^[7] effect is a promising approach to boost the system efficiency at reduced cost and is a subject of intensive research.

Various thermal refrigeration systems, reviewed in Sleiti et al.,^[8] can be powered with low-temperature heat sources such as absorption/adsorption systems,^[9–11] ejector systems,^[12,13] organic Rankine cycle (ORC) systems,^[12,14–16] and Stirling engine systems.^[17,18] Nevertheless, these systems have their own technical problems that limit their applications. For instance, the absorption/adsorption systems operate


1. Introduction

The worldwide demand for energy increases steadily alongside with the increased world population and modern life.^[1,2] Around 17% of the worldwide energy is consumed in cooling systems, while this percent in the gulf countries exceeds 67%.^[3,4] Furthermore, the negative impacts of the conventional energy resources make it necessary to minimize fossil fuel

efficiently at temperature sources higher than 90 °C. However, they have high initial cost, large size, and they experience corrosion problems. Ejector systems are simple, but their performance deteriorates at off-design conditions. The ORC is a proven technology, but ORC systems are not economical at heat source temperatures less than 100 °C.^[8] Also, the expanders used in the ORC are modified compressors with low efficiency and high cost (around 69% of the capital cost).^[8]

Sleiti et al.^[8] have presented a detailed review of the innovation approaches of thermomechanical refrigeration systems, including ejector systems, ORC systems, and isothermal and isobaric heat engines. They highlighted the major advantages of these systems over the other thermal refrigeration systems. Isothermal expansion heat engines, in particular, such as Stirling engines and Ericson engines, were introduced in several studies in the open literature to convert thermal energy to mechanical energy to drive electrical generators of refrigerant compressors.^[17,19,20] While these engines have the potential of reaching maximum theoretical efficiency, close to the Carnot efficiency, the actual manufactured engines have unsolved problems that prevent them from being commercialized. The actual efficiency of these engines is low due to the negative effect of the dead volumes, which also limits their output range. In addition, the use of gases as working fluids at very high pressure

Prof. A. K. Sleiti
Department of Mechanical and Industrial Engineering
College of Engineering
Qatar University
P.O. Box: 2713, Doha, Qatar
E-mail: asleiti@qu.edu.qa

 The ORCID identification number(s) for the author(s) of this article can be found under <https://doi.org/10.1002/ente.202000613>.

© 2020 The Authors. Energy Technology published by Wiley-VCH GmbH. This is an open access article under the terms of the Creative Commons Attribution License, which permits use, distribution and reproduction in any medium, provided the original work is properly cited.

The copyright line for this article was changed on 26 December 2020 after original online publication.

DOI: 10.1002/ente.202000613

makes the sealing very difficult. Even with low-output machines, the kinematic mechanism required to operate the dual pistons and the required high accuracy of single-piston Stirling engines make them very expensive. On the other hand, other expansion machines exert work by performing isobaric expansion with no polytropic expansion. The Worthington direct-acting steam pump^[21] and the Bush compressor^[22] are examples of these types of engines. The design of these machines' expanders is simpler than of those applying polytropic expansion, which reduces their cost. In addition, these engines are able to operate using heat directly, which makes them even more attractive for pumping and compression applications. An application of such an isobaric machine for refrigeration was presented by Sleiti et al.^[23] based on the work presented by Glushenkov et al.^[24] It consists of a novel thermomechanical expander-compressor unit (ECU) to drive a vapor compression refrigeration (VCR) system. The main advantages of this system are its ability to work with low-temperature heat sources of $\approx 70^\circ\text{C}$ and its simplicity, which minimizes its cost.

The main objective of the current study is to provide a database for suitable working fluids for these isobaric expansion engines based on their performance for a wide range of low heat source temperatures and a wide range of operating pressures. To achieve that objective, a large number of potential working fluids are studied and analyzed in a systematic fashion. One attractive and novel application introduced in this work is the utilization of these isobaric thermomechanical ECUs in refrigeration systems. This novel application is the first of its kind and is not to be confused with an ORC-driven refrigeration system found in the open literature^[25] as will be discussed and explained in subsequent sections.

The working fluids play a major role in the performance, design, and size of all components of the cycle. Several publications have investigated the working fluids of ORC systems based on efficiency, physical properties, safety, and environmental issues.^[26–32] Luo et al.^[26] have presented a systematic approach to evaluate large groups of refrigerants and mixtures for use in ORC systems to select the best fluids with low global warming potential (GWP). They mentioned that there is no single working fluid that satisfies every aspect of environmental, health, and safety (EHS) criteria, energy efficiency, and operating conditions. However, it is possible to find the best fluids by selecting fluid mixtures with different concentrations based on their design conditions. Rayegan and Tao^[28] have proposed a procedure to select working fluids for a solar ORC system. Among 117 organic fluids available in the Refprop 8.0 database, 11 fluids have been recommended to be used in solar ORC systems with low- or medium-temperature solar collectors.

Studies and investigations for a modified ORC system that replaces the polytropic expander with an isobaric expander are not available in the open literature. Bao and Zhao^[33] reviewed a working fluid and expander selections for an ORC system but not for isobaric expanders. Only one research study introduced the concept of using the isobaric ECU in a refrigeration system.^[25] However, their proposed model deals with the refrigerant vapor as an ideal gas, an assumption that could affect the results significantly. Also, they simulated the performance of only a few working fluids and one of them has been phased out (R12). In contrast, the current study investigates the performance of isobaric expansion machines

utilizing 36 preselected fluids from those available in the Engineering Equation Solver (EES) library. The investigation of these fluids is performed at low and ultralow heat source temperatures (40 to 300°C). Thus, the novelty of this work is that it is the first study that provides 1) comprehensive investigation of suitable working fluids for isobaric expansion machines for power and refrigeration applications; 2) classification of suitable fluids for thermal-power systems that use different low-grade heat waste sources at different temperatures and pressures; 3) a database of 36 working fluids for isobaric machines in terms of their efficiencies, back work ratio (BWR), and other important properties; and 4) a modified practical efficient design of the Worthington and Bush engines for refrigeration applications.

Waste heat is the rejected energy from a process at a temperature higher than the ambient temperature. Some of this energy can be recovered and used in other applications and the rest is rejected to the atmosphere or to the ground water, revisers, or oceans, causing thermal pollution. By recovering the waste heat, the amount of the usually consumed energy and its cost are reduced. In certain applications, using waste heat results in smaller energy conversion equipment and therefore results in even more cost savings; examples can be found in Wayne and Turner^[34] and in the *Annual Energy Reviews*.^[35] Waste heat temperatures can range from the ultralow 40°C to the very high 1650°C . In the current study, subranges are defined in terms of temperature range as provided in **Table 1**.

Herein, the focus is on the intermediate, low, and ultralow temperature range (T_H from 40 to 300°C). The use of waste heat in the low and ultralow temperature ranges, in particular, is the interest of the current study and while more problematic, it has huge untapped potential. We introduce an attractive application at the lower end of the range using a modified practical, efficient design of the Worthington- and Bush-type machines for refrigeration applications.

The work in this study is subdivided into five sections. Section 2 describes the isobaric machines (Worthington pump and Bush compressor) and their working principle. The thermodynamics model of these systems and the preselected fluids are presented in Section 3. Section 4 provides 1) discussions of the obtained results based on the fluid types and 2) comparison of the fluids' performances at various heat source temperatures for a wide range of pressure differences.

2. Description of Isobaric Expansion Machines

Isobaric expansion machines are devices that pump/compress fluid by performing an isobaric expansion process on their working fluids. The Worthington pump and the Bush compressor are the best known examples of these machines. In this

Table 1. Classification of waste heat sources by temperature range.

Temperature range	Low limit [$^\circ\text{C}$]	High Limit [$^\circ\text{C}$]
High	590	1650
Intermediate	200	590
Low	80	200
Ultralow	40	80

section, the configuration and working principles of these devices are explained.

2.1. Worthington Machines

Worthington's direct-acting simplex pump, the precursor of many others, was patented in 1849.^[36] The US Navy purchased the first Worthington pumps for the USS *Susquehanna* in 1850. Worthington's direct-acting duplex steam pump was patented in 1859. This pump ultimately became an industry standard. The USS *Monitor* pumps are probably the oldest surviving examples of Worthington's simplex design. In the current work, a new isobaric expansion engine design based on the Worthington machine and its basic working principle are shown in **Figure 1**. It consists of two cylinders (driver cylinder and compressor cylinder) with two rigid connected pistons that move as a unit inside the cylinders. The pumping process can be explained based on the pressure–volume diagram shown in **Figure 2**. The subscript “d” and “c” indicate the driver and compressor, respectively. First, during the power stroke, valve A is opened, while the other valves are closed. A highly pressurized fluid (at pressure of P_{d2}) is admitted through it and the pressure inside the driver cylinder increases from P_{d1} to P_{d2} (process 1–2). Then, the power stroke is completed at constant pressure P_{d2} (2–3). During processes 1–3, the volume of the expanded fluid is increased from almost zero to V_{d3} . Simultaneously, the pressure inside the compressor cylinder is increased from P_{c1} to P_{c2} (5–6). Then through the nonreturn valve B, the compressed fluid is discharged at pressure P_{c2} (6–7). During processes 5–7, the volume of the compressor chamber is decreased from V_{c1} to almost zero. After that, valve A is closed, and valve D is opened to discharge the driver fluid from the high pressure P_{d2} to the low pressure P_{d1} (3–4). In addition, during the backstroke, by the aid of the hydraulic accumulator (HA), the volume of the driver chamber is decreased from V_{d3} to almost zero volume. Simultaneously, the fluid of the compressor is admitted through valve C and the volume increases from almost zero to V_{c3} (8–5).

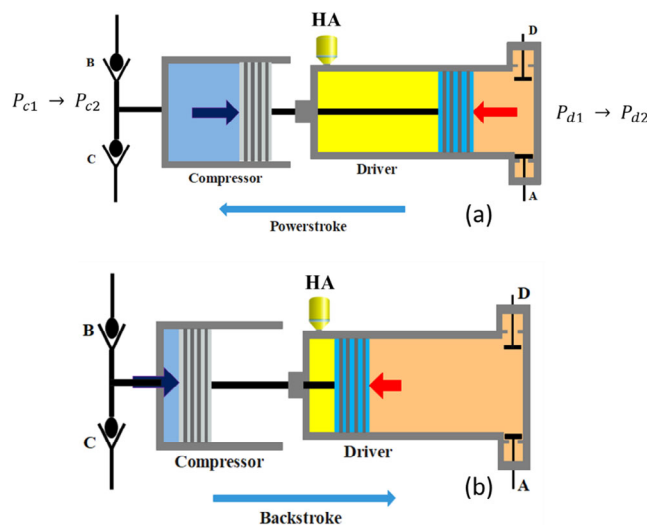


Figure 1. a) Powerstroke and b) backstroke of the Worthington pump.

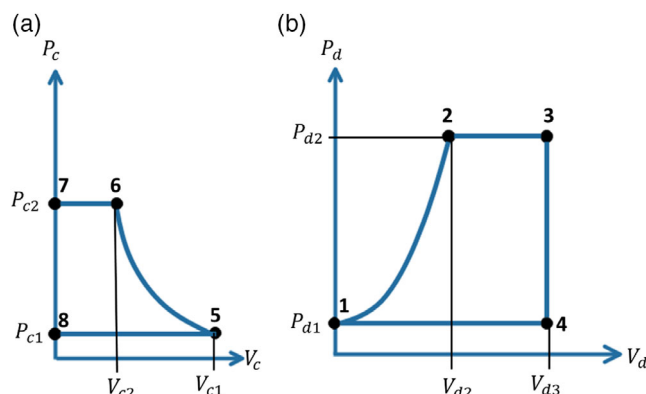


Figure 2. Working principle of the Worthington pump, a) power stroke and b) back stroke.

2.2. Bush-Type Engines

Figure 3 shows a new design (developed in this study) of the Bush-type engine used as a thermomechanical compressor unit integrated with the conventional VCR cycle. In this work, this system is referred to as a thermal-mechanical refrigeration (TMR) system. The engine (right-hand side in **Figure 3**) consists of a vertical cylinder with a piston connected to a spring mechanism. The piston divides the cylinder into hot and cold chambers. The working mechanism of the system can be explained as follows: 1) The spring keeps the piston in a reciprocating motion. 2) As the piston moves down, part of the liquid fluid is displaced from the cold side of the cylinder to the hot side. 3) The liquid evaporates and the pressure increases, displacing the other part of the liquid to the diaphragm unit. 4) The diaphragm unit compresses the vapor of the refrigerant (in the refrigeration loop) to the condenser through the upper nonreturn discharge valve. 5) The refrigerant vapor condenses in the condenser, expands through the expansion valve (EV), evaporates in the evaporator, and is redirected to the diaphragm unit.

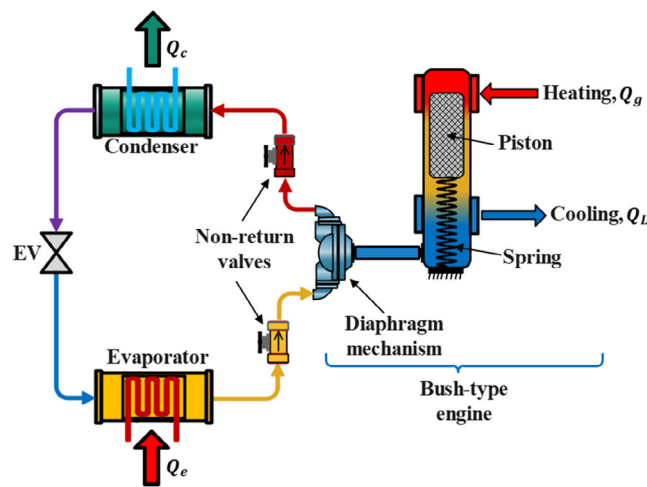


Figure 3. VCR system driven by Bush-type engine.

6) The low-pressure refrigerant vapor forces the liquid working fluid back to the cylinder while the piston is moving up. 7) Through the piston's moving-up stroke, it forces the hot working fluid (in gas phase) to return from the hot side to the cold side of the cylinder. Then the cycle repeats.

2.3. Comparison with Existing Systems

The proposed TMR technology is based on the use of an innovative prime mover (heat engine acting as compressor) that can be combined with VCR. The prime mover can be positioned in between ORC engines and Stirling-cycle thermal machines. From the technical point of view the engines by Bush,^[37] Malone (Sier, 2007), Manson, (Manson, 1952), and the Thermo-electron free-piston engine (Walker, 1980) have similar components as the heat-driven compressor. The thermodynamic cycles of the heat-driven compressor with dense working fluids as in the current study have never been used in heat engines. The technological solutions (mainly toward simplification of the design) are crucial components of the study novelty. Below, the TMR system is compared with existing solutions.

2.3.1. Stirling Engines

Robert Stirling applied for his first engine patent in 1816. The Seventeenth International Stirling Engine Conference which took place at Northumbria University, UK, on August 24–26, 2016, celebrated the Bicentennial Anniversary of the Stirling cycle. As the Stirling engine is truly unique in that it is the only practical example of a thermodynamically reversible machine, it has been the subject of extensive R&D for 200 years. Philips Research Laboratory in Eindhoven, General Motors Corporation of Detroit, and Ford Motor Co. of Detroit are among the companies that were concerned with Stirling engines for various applications. Despite clearly superior technical performance characteristics and all the efforts spent on development, modern Stirling engines are invariably not cost competitive from the

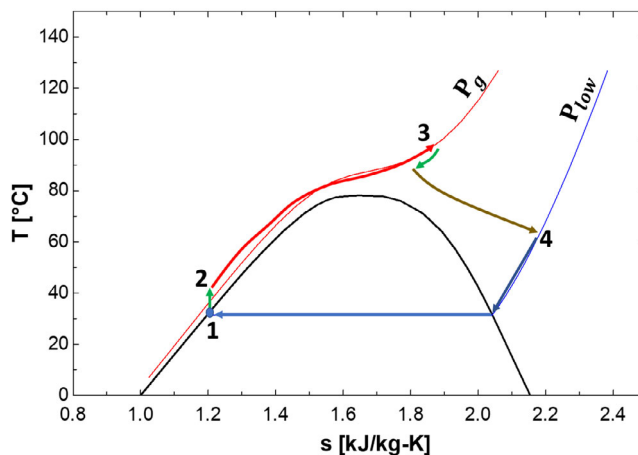


Figure 5. T - s diagram of the power loop of a refrigeration system driven by a Worthington pump.

standpoint of economical mass production. It seems that research on Stirling-cycle engines has expired (or almost expired). One of the reasons for this is that Stirling engines have been developed largely by adapting traditional methods and designs from the internal combustion engine technology. Today only a very special, high-temperature 1 kW free-piston design is available on the market (Microgen, <http://www.microgen-engine.com/>). This engine needs very high temperature (fuel combustion), it is difficult to scale and control the power, and it is very expensive, about \$10 000. A review by Wang et al.^[38] on Stirling cycle engines shows that this type of engine is still in the research phase. The novel engine as in the current proposal resembles to a certain extent a Stirling engine. However, it is radically different in the thermodynamic cycle and its technological implementation; examples are given in previous studies.^[17,24] A distinguishing feature of the engines in this study is their technical simplicity resulting in substantially lower cost and

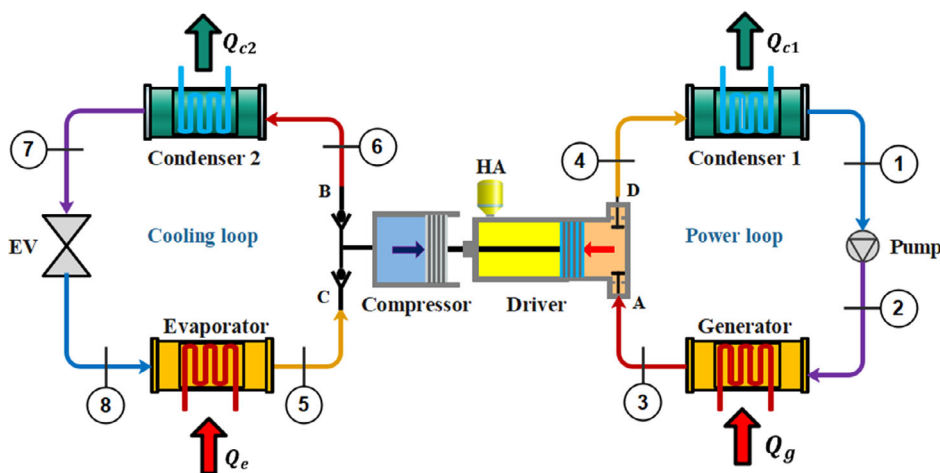


Figure 4. VCR system driven by Worthington-type engine.

higher energy efficiency (because of elimination of unnecessary energy losses).

2.3.2. ORC Engines

The ORC is the only proven and industrially applied technology to convert low-temperature heat into power. It is considered to be the most efficient and economic technology in temperature

ranges of 200–400 °C.^[39] An assessment of the potential of various heat recovery technologies by Hammond and Norman^[40] showed that the greatest potential for reusing the surplus heat available is, in particular, in conversion to electricity, mostly using ORC technology. However, the specific costs of 2000–4000€ kW⁻¹^[41] is rather high. At ultralow heat source temperatures, below 100 °C, the technology is not economic at all. The Kalina cycle, a variation of the classical ORC utilizing

Table 2. Preselected working fluids.

Fluid	Type	Toxicity	Flammability	GWP	Normal boiling point [°C]	P_{cr} [bar]	T_{cr} [°C]	ν_3^a [m ³ kg ⁻¹]	BWR ^a [%]	η^a [%]	P_{sat} [bar]
Propane	Alkane	A	3	20	-42.25	42.5	96.7	0.0487	4.2	1.1	10.79
n-Butane		A	3	20	-1.00	38.0	152.0	0.1175	1.5	2.6	2.84
n-Pentane		A	3	11	36.00	33.6	196.5	0.1921	0.8	4.2	0.83
n-Hexane		NA	3	NA	69.00	30.6	234.7	0.0017	92.6	0.0	0.25
n-Heptane		NA	3	NA	98.38	27.3	267.0	0.0016	93.5	0.0	0.08
Isobutane		A	3	20	-12.00	36.4	134.7	0.0910	2.0	2.1	4.05
Neopentane		A	3	20	10.00	32.0	160.6	0.1225	0.7	3.1	2.01
isopentane		A	3	20	28.00	33.7	187.2	0.1745	0.9	4.0	1.09
Isohexane		NA	3	NA	60.00	30.4	224.6	0.0017	92.4	0.0	0.35
Cyclopentane	Cycloalkane	A	3	NA	49.20	45.7	238.6	0.1983	0.7	4.2	0.51
Cyclohexane		A	3	NA	80.74	40.8	280.5	0.0014	93.7	0.0	0.16
Propylene	Alkene	A	3	NA	-47.60	46.7	92.4	0.0402	5.0	0.9	13.07
Butene		NA	3	NA	-7.00	40.1	146.1	0.0962	0.1	2.2	3.44
Isobutene		A	3	20	-6.90	40.1	144.9	0.0962	1.8	2.2	3.54
Benzene		NA	3	NA	80.10	48.9	288.9	0.0012	93.7	0.0	0.16
Methanol	Alcohol	NA	3	NA	64.70	81.0	240.2	0.0014	93.7	0.0	0.21
Ethanol		NA	3	NA	78.00	62.7	241.6	0.0014	94.1	0.0	0.11
Acetone	Ketone	NA	3	NA	56.00	47.0	235.0	0.2337	0.5	4.0	0.38
Dimethylether	Ether	NA	4	NA	-24.00	53.7	127.2	0.0728	2.1	1.5	6.84
Diethylether		NA	4	NA	34.60	36.4	193.6	0.1876	0.8	4.2	0.86
Dimethyl carbonate	Carbonate ester	NA	4	NA	90.00	49.1	284.2	0.0010	93.2	0.0	0.09
Ammonia	Pnictogen hydride	B	2	1	-33.00	113.3	132.3	0.1228	0.3	1.0	11.67
Water					100.00	220.6	373.9	0.0010	97.6	0.0	0.04
Hexamethyldisiloxane		A	3	NA	0.00	19.4	245.5	0.0014	93.3	0.0	0.08
Novoc649		NA	NA	1	49.00	18.7	168.7	0.0422	1.5	3.1	0.50
R32	HFC	A	2	675	-52.00	57.8	78.1	0.0229	4.7	0.7	19.28
R134a	HFC	A	1	1300	-26.00	40.6	101.0	0.0286	2.9	1.3	7.71
R227ea	HFC	A	1	257	-16.00	29.3	101.8	0.0220	3.3	1.4	5.28
R245fa	HFC	B	1	925	15.00	36.5	154.0	0.0686	1.1	2.9	1.77
R1234yf	HFO	A	2L	4	-29.00	33.8	94.7	0.0253	3.7	1.3	7.84
R152a	HFC	A	2	120	-24.00	45.2	113.3	0.0440	2.6	1.3	6.91
R161	HFC	A	3	12	-37.00	50.1	102.1	0.0452	3.2	1.1	10.56
RC318	PFC	A	1	8700	-6.00	27.8	115.2	0.0268	2.5	1.8	3.66
R218	PFC	A	1	8830	-36.70	26.4	71.9	0.0116	6.7	0.9	9.96
RE245Fa2	HFC	B	1	950	15.00	34.3	171.7	0.0731	1.0	3.3	1.04
RE245cb2	HFC	NA	NA	NA	5.61	28.9	133.7	0.0446	1.8	2.2	2.43

^a) At $T_H = 80$ °C and $\Delta P = 1$ bar.

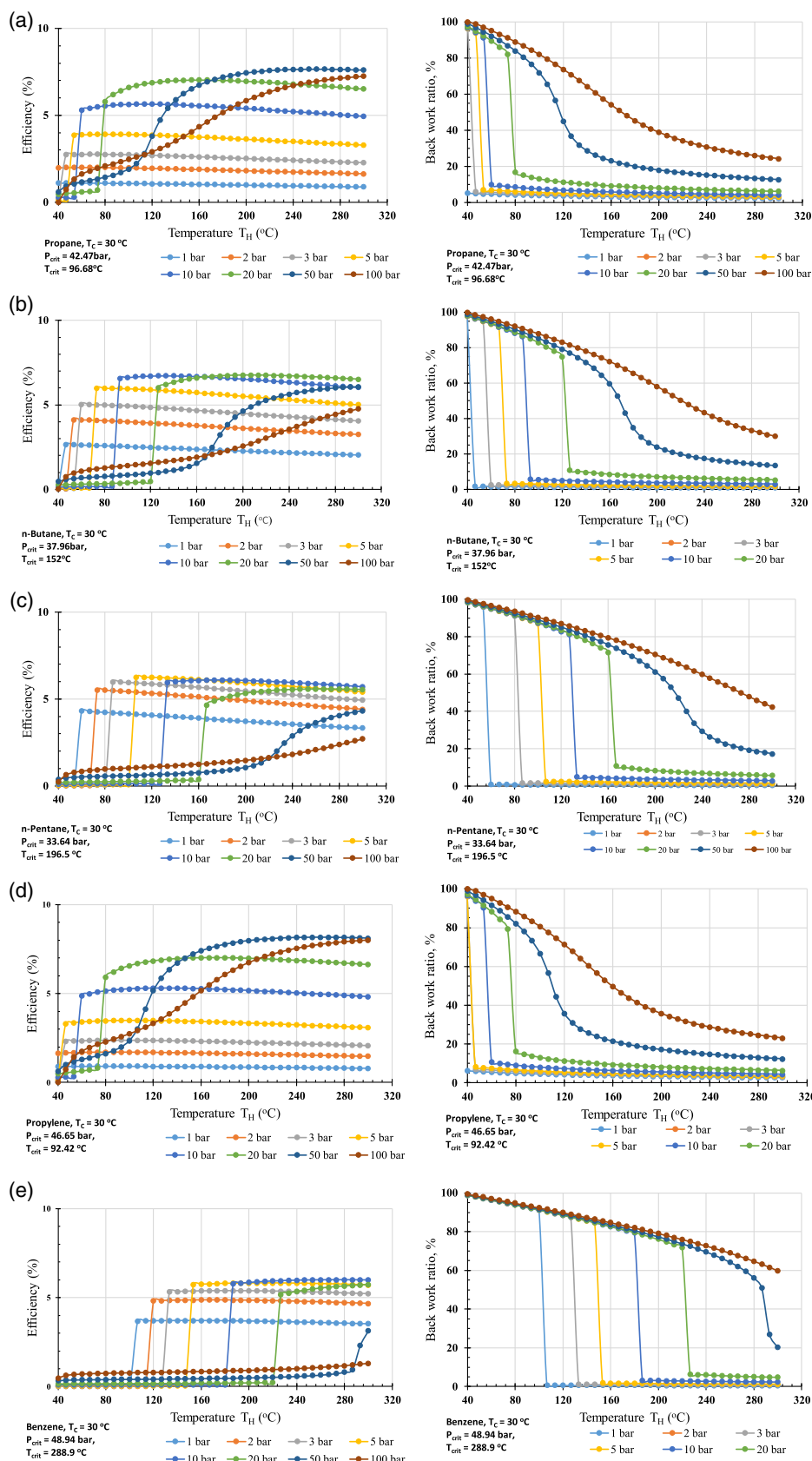


Figure 6. Efficiency and BWR of a) propane, b) n-butane, c) n-pentane, d) propylene, and e) benzene.

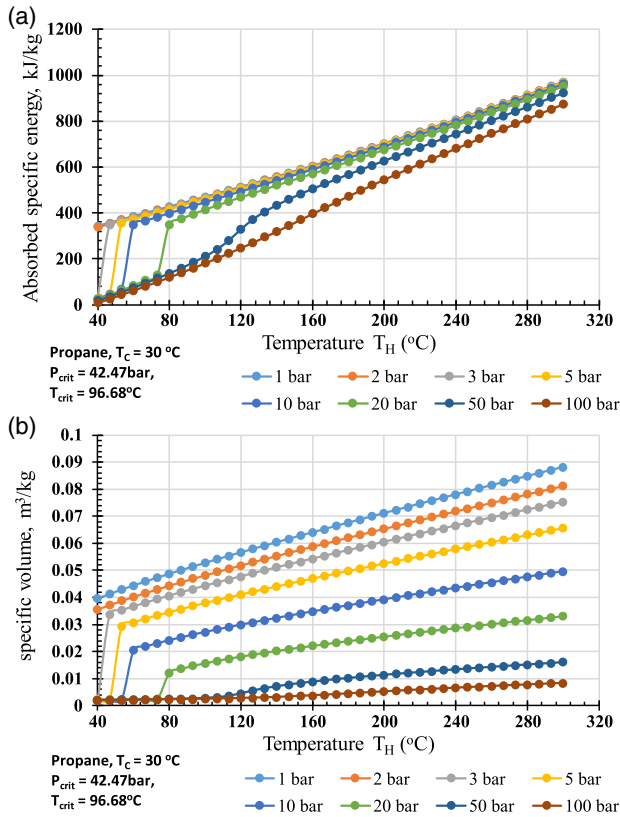


Figure 7. Variation of a) absorbed heat in the generator and b) specific volume at the inlet of the driver chamber with heat source temperature and pressure difference.

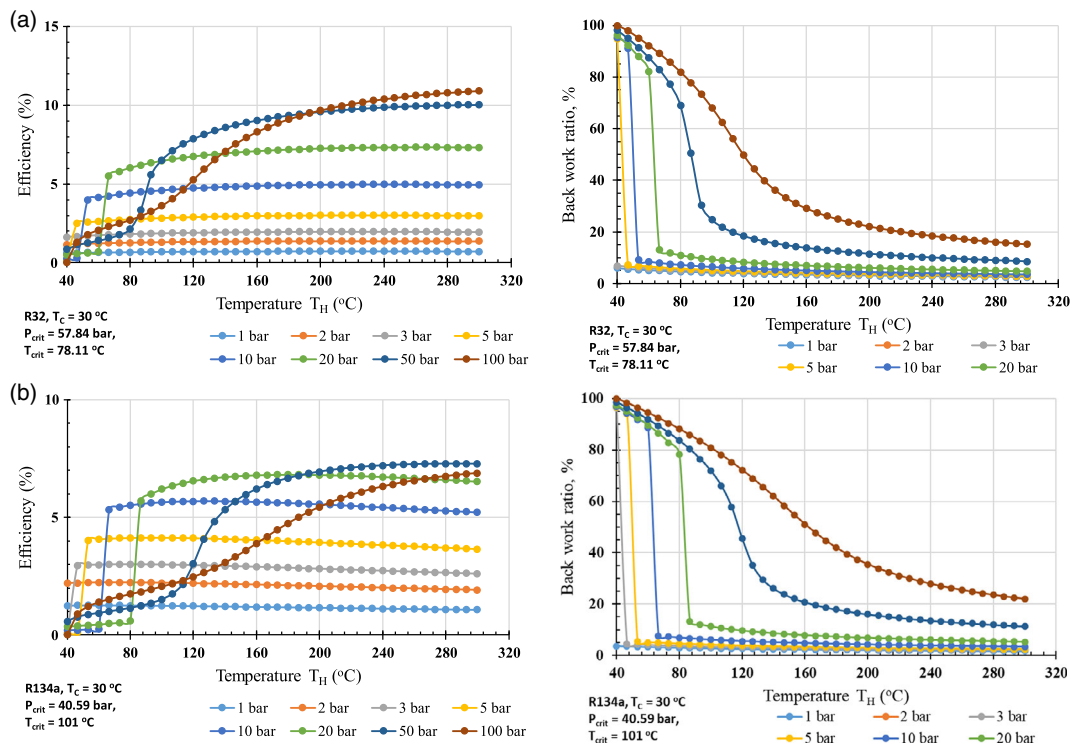


Figure 8. Efficiency and BWR of a) R32 and b) R134a.

water–ammonia mixtures, is a promising alternative for very low temperature sources.^[42] However, studies indicate that the promised benefits of Kalina cycles appear overestimated, while this process is much more complex and maintenance demanding than classical ORC processes.^[43]

3. Experimental Section

In this section, the thermodynamics models developed to investigate the performance of the isobaric machines are described. The performance of these machines is introduced in terms of their energy efficiency and BWR.

3.1. Modeling of Worthington Machine Integrated with VCR System

The Worthington pump can be used to compress the working fluid of a refrigeration system as mentioned in the previous sections and shown in **Figure 4**. In the power loop, the pump compresses the working fluid from the low pressure of condenser 1 (state 1) to the high pressure of the generator (state 2). In the generator, the working fluid is evaporated utilizing a low-grade heat source up to superheated or supercritical state (state 3). Valve A is opened, and the highly pressurized fluid is admitted, compressing the working fluid of the cooling loop during the power stroke. The operating mechanism of the Worthington pump is explained in Section 2.1. Through the back stroke, the working fluid of the power loop is discharged again to the condenser pressure to be condensed and repeats the cycle.

The maximum efficiency of the power loop can be expressed as

$$\eta = \frac{W_{\text{net}}}{Q_{\text{g}}} \quad (1)$$

where Q_{g} is the energy absorbed by the generator from the heat source and W_{net} is the new work developed by the driver on the compressor chamber, which can be estimated as

$$W_{\text{net}} = W_{\text{d}} - W_{\text{p}} \quad (2)$$

where W_{d} is the work produced by the piston of the driver cylinder during the power stroke, which is given (as a maximum) in terms of the generator pressure P_{g} , condenser pressure P_{c1} , mass of the working fluid in each stroke m , and the specific volume at the outlet of the generator v_3 as

$$W_{\text{d}} = m(P_{\text{g}} - P_{\text{low}})v_3 \quad (3)$$

while the pumping work is given as

$$W_{\text{p}} = m(h_2 - h_1) \quad (4)$$

where h_1 and h_2 are the specific enthalpies of the working fluid at states 1 and 2, respectively. Also, the energy added to the generator is given in terms of enthalpies at point 3 (h_3) and point 2 (h_2) as

$$Q_{\text{g}} = m(h_3 - h_2) \quad (5)$$

Another indicator that can be used to evaluate the performance of the isobaric machines is the BWR, which is defined

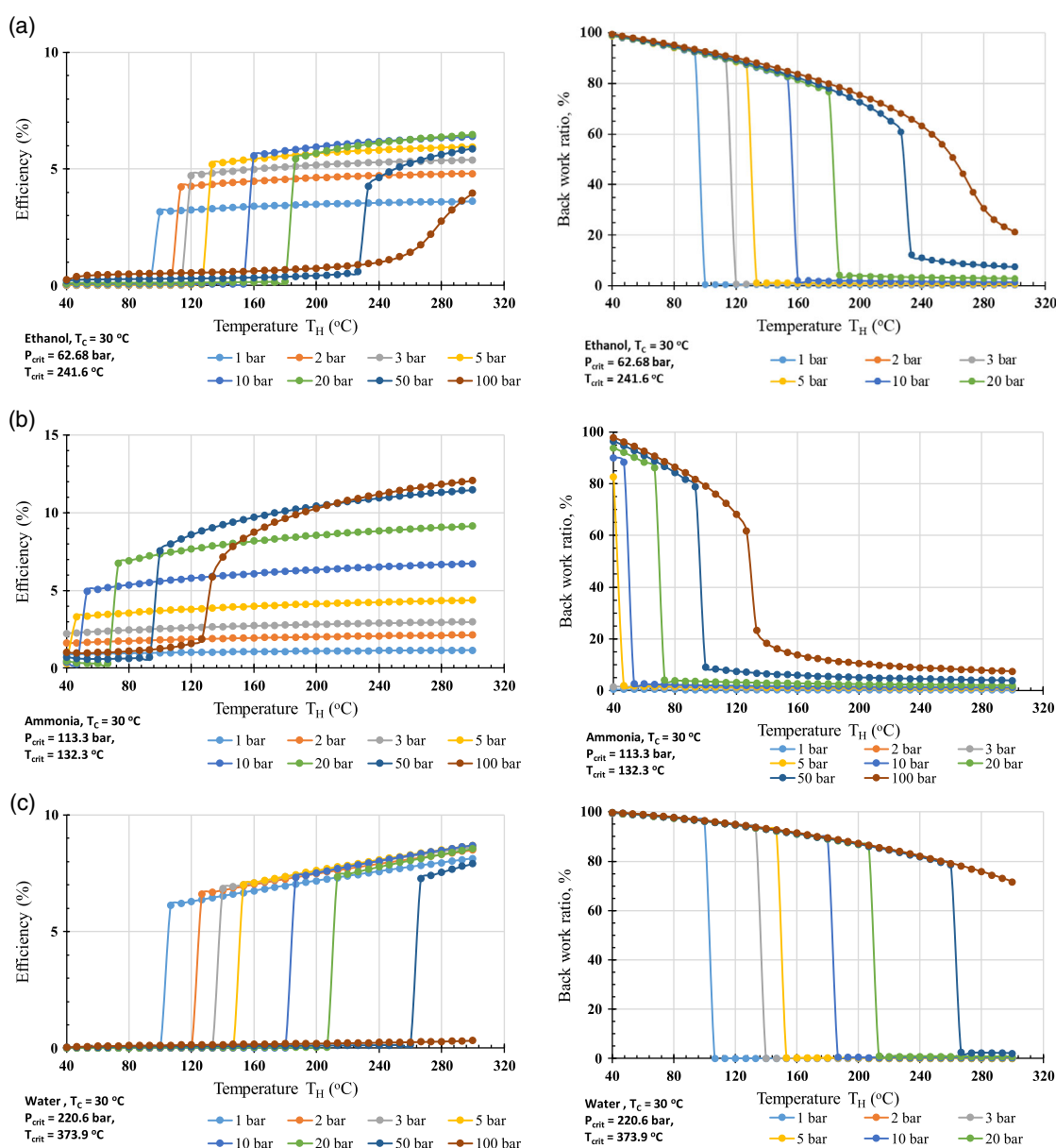


Figure 9. Efficiency and BWR of a) methanol, b) ammonia, and c) water.

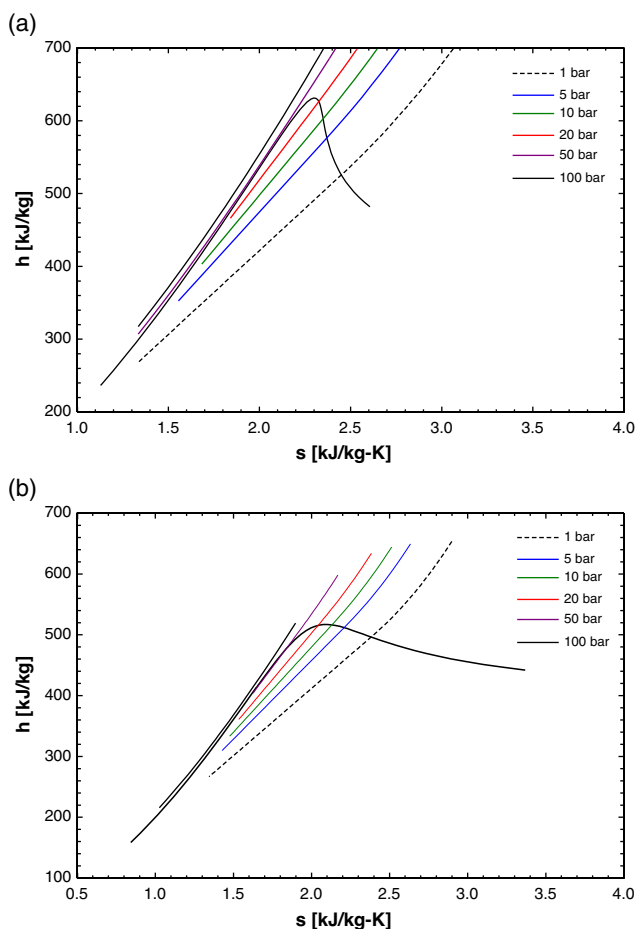


Figure 10. h - s diagram for a) propane and b) R32.

as the ratio of the pumping energy consumed by the pump to the maximum energy produced by the driver as

$$\text{BWR} = \frac{W_p}{W_d} \quad (6)$$

It should be mentioned that the thermodynamics properties of the working fluid were obtained at the mentioned states in Figure 4 and presented in the T - s diagram as shown in Figure 5 as follows. 1) State 1: ($P = P_{\text{low}}, T = T_C$) where P_{low} was selected to be slightly higher than the saturated pressure at the low temperature ($T_C = 30^\circ\text{C}$) or set at 1 bar to avoid the undesirable boiling at the inlet of the pump. 2) State 2: $P = P_g, T_2 = T$ ($P = P_g, s = s_1$). 3) State 3: $P = P_g, T = T_H$.

3.2. Modeling of the Bush-Type Engine

Similar to the Worthington-type engine, the efficiency of the Bush-type engine (Figure 3) is expressed as the ratio of the useful work generated during the cycle (Equation 7) to the energy absorbed by the hot chamber (Equation 8)

$$W = \oint p dV_{\text{tot}} = \oint p dV_H + \oint p dV_C \quad (7)$$

$$\begin{aligned} Q_H &= \oint dU_H + \oint p dV_H + \oint h^{\text{out}} dm_H^{\text{out}} - \oint h^{\text{in}} dm_H^{\text{in}} \\ &= \oint dU_H + \oint p dV_H + \Delta Q_H \end{aligned} \quad (8)$$

where the total volume V_{tot} includes the volume of the hot chamber V_H , volume of the cold chamber V_C , and volume of the regenerator V_R (when regeneration is considered). ΔQ_H is the energy required to heat the displaced working fluid from the low cycle temperature T_C to the high cycle temperature T_H . The term $\Delta Q_H = \oint h^{\text{out}} dm_H^{\text{out}} - \oint h^{\text{in}} dm_H^{\text{in}}$ in the above equation defines the performance of the regenerator. More details of the thermodynamics modeling of the Bush-type engine can be found in previous studies.^[23,44]

It was observed that the results (efficiency and BWR) for the two engines are comparable because they are similar in size, operation principles, and input parameters; however, they are different in other technical terms. So, only the results of working fluid investigation based on the model of the Worthington engine type are presented in this study for brevity.

3.3. Preselection Criteria and Fluid Description

The main objective of this study is to evaluate the performance of isobaric expansion machines/engines utilizing various working fluids. A choice of compressor working fluid is defined in many respects by the heat source temperature. The working fluids that suit the best for the engine thermodynamic cycle in the temperature range of 50–150 °C will be selected. Also, fluids with high performance in the temperature range of 150–300 °C will be highlighted. In the preselection process of the working fluids, several criteria are considered. The fluids should have high thermal expansion per kilowatt heat supplied and low compressibility in the liquid phase. The dependence of enthalpy on the pressure and temperature that is favorable for efficient regeneration is the most important requirement toward the working fluid properties. Moreover the working fluid should be nontoxic, environmentally acceptable (GWP and ozone depleting potential (ODP)), stable, and not corrosive. Based on these criteria, a total of 166 fluids were investigated and those that did not meet the criteria were eliminated. The fluids shown in Table 2 were selected to be investigated further in this study. The fluids in Table 2 are listed according to their type (11 types). Most of these fluids belong to the alkane/cycloalkane/alkene and hydrofluorocarbon (HFC) families. IUPAC defines alkanes as “acyclic branched or unbranched hydrocarbons having the general formula C_nH_{2n+2} , and therefore consisting entirely of hydrogen atoms and saturated carbon atoms.” Compared to the HFC family, alkanes/cycloalkanes/alkenes have higher critical temperatures and comparable critical pressures with lower GWP. HFC refrigerants are the third generation of fluorinated refrigerants. Recognized as ODP and GWP, they represent a better alternative to chlorofluorocarbon and hydrochlorofluorocarbon. Refrigerants in this group are applicable to refrigeration plants and air conditioning units

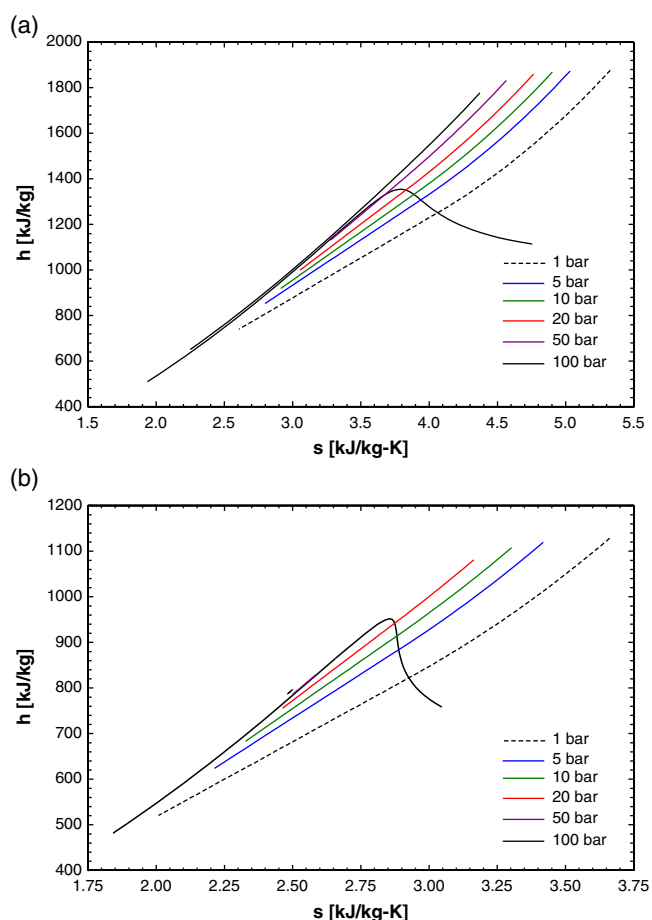


Figure 11. h - s diagram of a) ethanol and b) acetone.

designed specifically for their use. The last three columns in Table 2 (v_3 , BWR, and η) will be discussed in the results section.

4. Results and Discussion

The models of Worthington-type and Bush-type engines described previously were implemented in EES to study the effects of different operating temperatures and pressures on the efficiency and BWR of both engine types for the selected working fluids. In the results obtained for different types of fluids discussed subsequently, the minimum cycle temperature (temperature of the heat sink) was taken as $T_C = 30^\circ\text{C}$ for all working fluids. The maximum/high cycle temperature (heat source temperature, T_H) was varied from 40°C to 300°C to estimate the potential of this technology for low- and intermediate-temperature applications. The range of difference between the high and low pressure, $\Delta P = (P_h - P_{low})$, was varied from 1.0 to 100 bar.

4.1. Efficiency and BWR of Different Types of Fluids

In this section, the performance of the selected fluids based on their types is discussed. As mentioned before, the performance

of the isobaric machines is presented in terms of the efficiency and BWR.

4.1.1. Alkanes and Alkene Fluids

Figure 6 shows the efficiency and BWR of selected fluids that belong to alkanes and alkene families for $T_C = 30^\circ\text{C}$, T_H range from 40 to 300°C , and the $\Delta P = (P_h - P_{low})$ range of 1.0 to 100 bar. It can be noted that the efficiency increases with the increase of the pressure difference up to a certain value (depending on the fluid), then starts to decrease with further increase in the pressure difference. For instance, in Figure 6a, the efficiency stabilizes around 1% at $\Delta P = 1$ bar. At $\Delta P = 2$ bar, it stabilizes at 2% and so on up to $\Delta P = 10$ bar. However, at $\Delta P = 20$ bar, the efficiency is higher than at $\Delta P = 50$ bar with $T_H < 160^\circ\text{C}$. It is also higher than at $\Delta P = 100$ bar with $T_H < 240^\circ\text{C}$. Furthermore, the efficiency of $\Delta P = 50$ bar is higher than that of $\Delta P = 100$ bar with $T_H > 112^\circ\text{C}$.

Similar behavior is noted for the other fluids with optimum pressure achieved at different temperatures. Also, the efficiency at low pressure differences slightly reduces with the increase of the heat source temperature. This is explained by the decrease of the specific volume v_3 at the inlet of the driver having more effect than the decrease of the absorbed energy in the generator, as shown in Figure 7a,b, respectively. Furthermore, the BWR increases with the increase of the pressure difference and decreases with the increase of the heat source temperature. It starts at a very high percentage due to the high consumed energy in the pump compared to the produced energy by the driver. This is explained by the liquid phase of the fluid at the low temperatures of the heat source. Comparing the efficiencies of the fluids in Figure 6 with each other, it can be noted that the achieved efficiency at the same heat source temperature and pressure difference differs considerably.

For instance, at $\Delta P = 5$ bar and heat source temperature of $T_H = 80^\circ\text{C}$, the obtained efficiency by propane is 5.8% (Figure 6a), by n-butane is 5.98% (Figure 6b), by n-pentane is 0.063% (Figure 6c), by propylene is 3.46% (Figure 6d), and by benzene is 0.042% (Figure 6e). This means that both propane and n-butane can work at low temperatures and low pressure differences. Whereas other fluids need a higher temperature with an optimum pressure difference to achieve efficiencies higher than 5%, it should be noted that for this family (except benzene), an optimum efficiency of 7% is achieved at the heat source temperature of 160°C and pressure difference of 20 bar. Regarding the other selected fluids of this family (which are shown in Table 1), it is found that the obtained efficiencies of isobutene are similar to those of n-butane, those of neopentane are similar to those of n-pentane, and those of propylene are similar to those of propane.

4.1.2. HFC Fluids

Overall, among the 36 fluids investigated in this study, only two fluids achieved efficiencies higher than 10% at high pressure difference, which are R32 and ammonia as shown in Figure 8a and 9b, respectively. This can be explained by the change in the energy added to the generator at higher pressures. It is noted

that the decrease of the energy added to the generator in case of R32 is much higher than in the case of propane, as shown in the $h-s$ diagram in **Figure 10**. For instance, at a mass of 1 kg per stroke, the energy added to the generator at $\Delta P=1$ bar is 970 kJ for propane and 584 kJ for R32.

The other selected fluids of the HFC family have performance comparable to those of the alkane family. However, the alkane family fluids contain highly flammable components, which limits their applications for refrigeration. In contrast, the HFC refrigerants have low flammability.

4.1.3. Other Selected Fluids

Comparing the obtained results of the other investigated fluids, it is found that the results of ethanol are similar to those of methanol and acetone (see **Figure 9a**). The similarity of the results is caused by the similar amount of energy added to the generator as the pressure difference increases, as shown by the $h-s$ curves of

ethanol and acetone (see **Figure 11**). While water has the most favorable environmental properties, it has poor performance in these types of engines (isobaric engines); see **Figure 9c**. As mentioned before, ammonia was able to achieve efficiencies higher than 10% at high pressure difference, as shown in **Figure 9b**.

4.2. Classification of Working Fluids according to T_H and ΔP

In this section, the working fluids are classified into five categories. Category I is those fluids with high performance at the heat source temperature (T_H) of 80 °C. Categories II, III, IV, and V are the high-performing fluids for T_H of 100, 140, 180, and 300 °C, respectively. The overall behavior, in terms of the efficiency of the fluids, is discussed first in Section 4.2.1, then the classification of the fluids according to T_H categories and for the ΔP range from 1 bar to 100 bar is provided in Section 4.2.2.

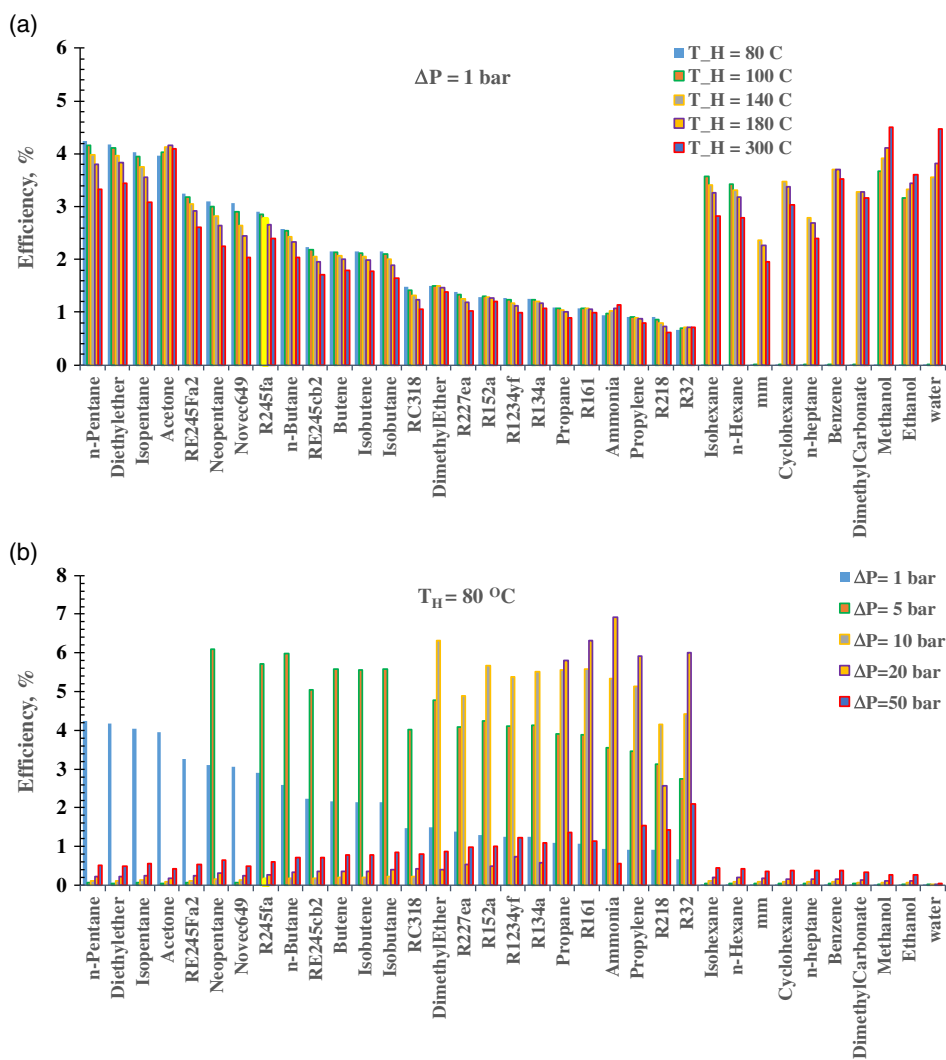


Figure 12. Efficiencies of the selected fluids at specified pressure differences and heat source temperature, $T_H = 300$ °C.

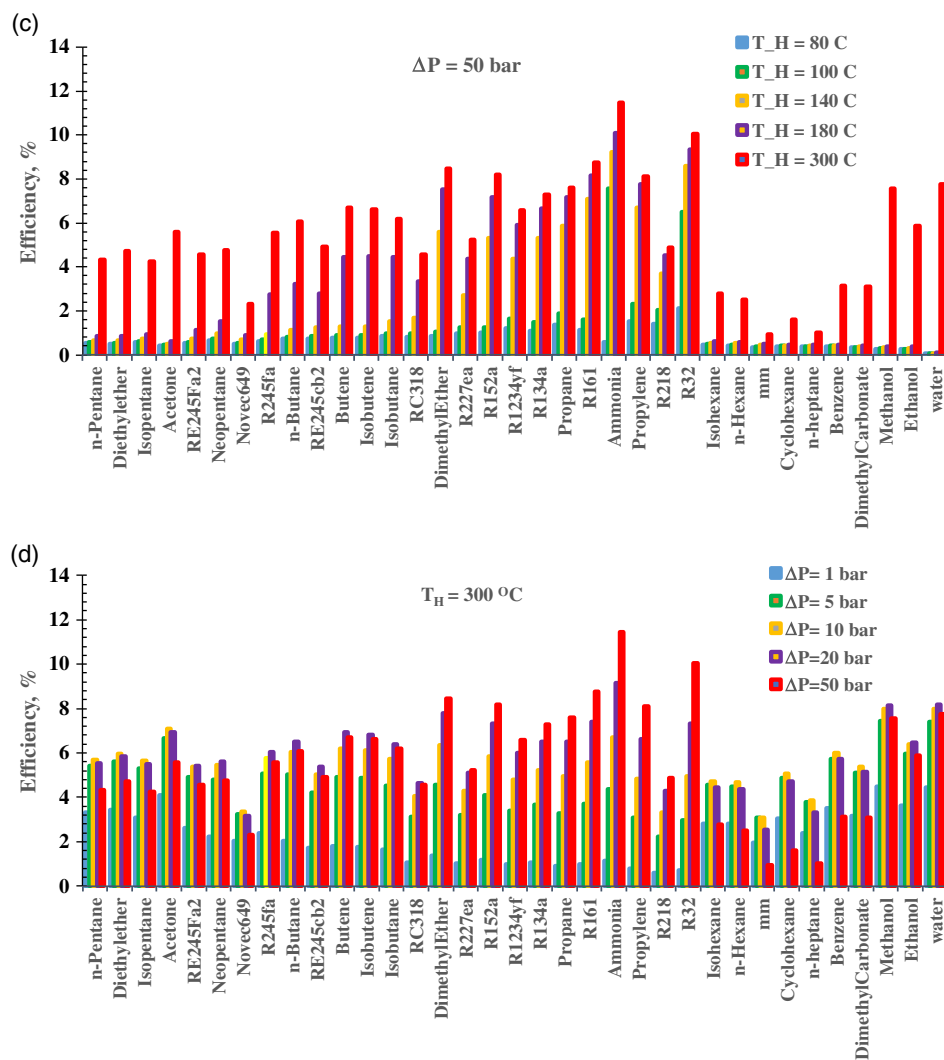


Figure 12. Continued.

4.2.1. Overall Performance Behavior of the Fluids in Terms of Efficiency

Figure 12 shows the efficiency of the 36 selected fluids at different pressure differences (ΔP) and heat source temperatures (T_H). The order of the fluids on the x-axis of Figure 12a was based on the values of the fluids' efficiency (from the highest to the lowest) at $\Delta P = 1 \text{ bar}$ and $T_H = 80 \text{ °C}$. This order of fluids is then kept for subsequent results and discussion. In general, it was found that at $\Delta P = 1 \text{ bar}$, the efficiency decreases with the increase of the heat source temperature. This behavior is reversed for the last three fluids (methanol, ethanol, and water) at the same conditions (Figure 12a). Furthermore, when the pressure difference is increased to $\Delta P = 50 \text{ bar}$ (Figure 12c), the efficiency increases with the increase of the heat source temperature for all selected fluids. However, at $T_H = 300 \text{ °C}$ and various pressure differences, the behavior of the efficiency curves (Figure 12c) is not as uniform as that at various temperatures

(Figure 12d). Comparing the behavior of efficiency curves in Figure 12a,b, it can be concluded that the driver efficiency is less sensitive for the temperature variation than for the pressure variation.

Also, it can be noted from Figure 12b that the efficiency of some fluids at medium pressure differences with $T_H = 80 \text{ °C}$ is higher than at very low or very high pressure differences. For instance, ammonia has an efficiency of 0.94% and 0.56% at $\Delta P = 1 \text{ bar}$ and $\Delta P = 50 \text{ bar}$, respectively, whereas at $\Delta P = 20 \text{ bar}$, its efficiency jumps to 7% (at $T_H = 80 \text{ °C}$). At $\Delta P = 50 \text{ bar}$ and $T_H = 300 \text{ °C}$, ammonia and R32 obtained the highest efficiencies, as noted before, over the other selected fluids (11.5% for ammonia and 10% for R32).

4.2.2. Classification of the Fluids according to T_H Categories for 1–50 bar ΔP Range

In this study, the working fluid is considered suitable for isobaric engines when its efficiency exceeds 5%; below that

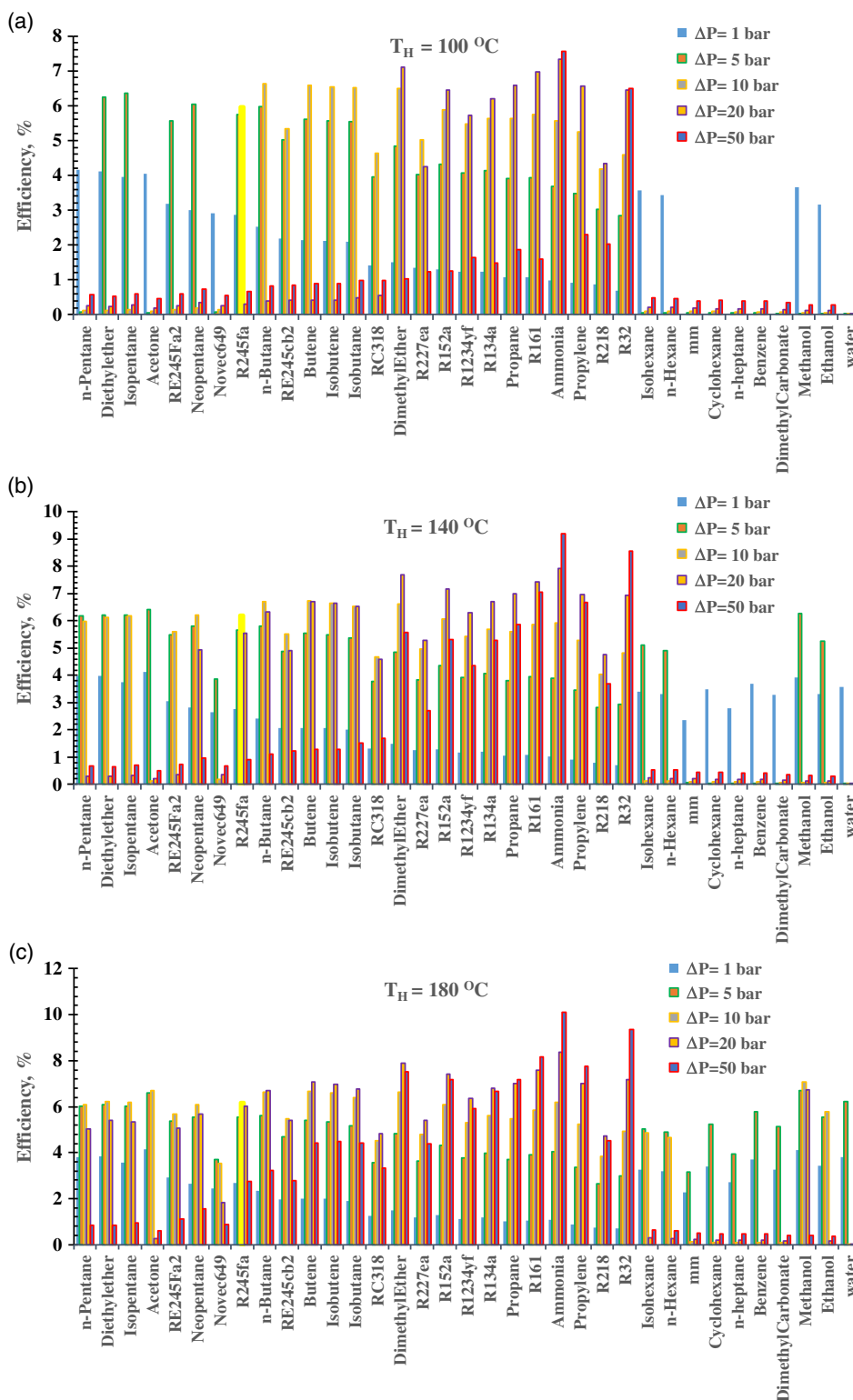


Figure 13. Efficiencies of the selected fluids for ΔP of 1–50 bar at T_H of a) 100 °C, b) 140 °C, and c) 180 °C.

the system will cease being economically viable and the fluids will not be recommended. **Figure 13** shows the efficiency of all 36 fluids for $T_H = 100, 140,$ and 180 °C, while for

$T_H = 80$ and for $T_H = 300$ °C, the efficiencies are provided in **Figure 12**. The fluid classification results are summarized in **Table 3** and **4**.

Table 3. Efficient fluids for ΔP of 1–50 bar for category I ($T_H = 80^\circ\text{C}$), II ($T_H = 100^\circ\text{C}$), and III ($T_H = 140^\circ\text{C}$).

T_H [$^\circ\text{C}$]	Fluid	η [%]	ΔP [bar]	T_H [$^\circ\text{C}$]	Fluid	η [%]	ΔP [bar]	T_H [$^\circ\text{C}$]	Fluid	η [%]	ΔP [bar]	
80	<i>n</i> -Pentane	4.2	1	100	None	NA	1	140	None	NA	1	
	Diethylether	4.2	5		Diethylether	6.2	5		<i>n</i> -Pentane	6.2	5	
	R245fa	5.7			Isopentane	6.4	Diethylether		6.2	Isopentane	6.2	
	<i>n</i> -Butane	6.0			RE245Fa2	5.6	Isopentane		6.2	Acetone	6.4	
	RE245cb2	5.0			Neopentane	6.0	Methanol		6.3	<i>n</i> -Pentane	6.0	10
	Butene	5.6			R245fa	5.7	<i>n</i> -Pentane		6.0	Diethylether	6.1	
	Isobutene	5.6			<i>n</i> -Butane	6.0	Diethylether		6.1	Isopentane	6.2	
	Isobutane	5.6			RE245cb2	5.0	Isopentane		6.2	Neopentane	6.2	
	Dimethylether	4.8			Butene	5.6	Neopentane		6.2	R245fa	6.2	
	R152a	4.2			Isobutene	5.6	R245fa		6.0	<i>n</i> -Butane	6.7	
	Dimethylether	6.3			Isobutane	5.5	<i>n</i> -Butane		6.6	Butene	6.7	
	R227ea	4.9			R245fa	6.0	RE245cb2		5.3	Isobutene	6.7	
	R152a	5.7			<i>n</i> -Butane	6.6	Butene		6.6	Isobutane	6.5	
	R1234yf	5.4			RE245cb2	5.3	Isobutene		6.5	Dimethylether	6.6	
	R134a	5.5			Butene	6.6	Isobutane		6.5	R152a	6.1	
	Propane	5.6			Isobutene	6.5	Isobutane		6.5	<i>n</i> -Butane	6.3	20
	R161	5.6		Isobutane	6.5	Dimethylether	6.5	Butene	6.7			
	Ammonia	5.3	Dimethylether	6.5	R227ea	5.0	Isobutene	6.7				
	Propylene	5.1	R227ea	5.0	R152a	5.9	Isobutane	6.5				
	R218	4.2	R152a	5.9	R1234yf	5.5	Dimethylether	7.7				
	R32	4.4	R1234yf	5.5	R134a	5.6	R152a	7.2				
	Propane	5.8	R134a	5.6	Propane	5.6	R1234yf	6.3				
	R161	6.3	Propane	5.6	R161	5.7	R134a	6.7				
	Ammonia	6.9	R161	5.7	Ammonia	5.6	Propane	7.0				
	Propylene	5.9	Ammonia	5.6	Propylene	5.3	R161	7.4				
	R32	6.0	Propylene	5.3	Dimethylether	7.1	Ammonia	7.9				
	None	NA	50	Dimethylether	7.1	20	R161	7.4				
				R152a	6.4	Ammonia	7.9					
				R1234yf	5.7	Propylene	7.0					
				R134a	6.2	R32	6.9					
				Propane	6.6	R161	7.1	50				
				R161	7.0	Ammonia	9.2					
Ammonia				7.3	Propylene	6.7						
Propylene				6.6	R32	8.6						
R32				6.5								
Ammonia				7.5	50							
R32				6.5								

Based on Figure 12 and 13 and Table 3 and 4, the following noticeable observations are made. Ammonia and R32 have the highest efficiencies at high ΔP of 50 bar for the T_H range 100–300 $^\circ\text{C}$. R161 has high performance for ΔP higher than 10 bar up to $\Delta P = 50$ bar for the full range of T_H from 80 to 300 $^\circ\text{C}$. This finding is very important as it makes R161 the choice fluid for a wide range of applications.

For category I ($T_H = 80^\circ\text{C}$), the best performer is ammonia at $\Delta P = 20$ bar, followed by R161 at the same $\Delta P = 20$ bar, dimethyl

ether at $\Delta P = 10$ bar, and *n*-butane at $\Delta P = 5$ bar, respectively. For category II ($T_H = 100^\circ\text{C}$), category III ($T_H = 140^\circ\text{C}$), and category IV ($T_H = 180^\circ\text{C}$), the best performers are ammonia, dimethyl ether, and R161, respectively all at $\Delta P = 20$ bar. For category V ($T_H = 300^\circ\text{C}$), the best performers, in addition to ammonia, dimethyl ether, and R161, are methanol and water at $\Delta P = 20$ and 50 bar. In general, fluids that have high specific volume, v_3 (see Table 2) or low density at the given T_H and ΔP , show higher efficiency and lower BWR.

Table 4. Efficient fluids for ΔP of 1–50 bar for category VI ($T_H = 180^\circ\text{C}$) and V ($T_H = 300^\circ\text{C}$).

T_H [$^\circ\text{C}$]	Fluid	η [%]	ΔP [bar]	T_H [$^\circ\text{C}$]	Fluid	η [%]	ΔP [bar]
180	None	NA	1	300	None	NA	1
	<i>n</i> -Pentane	6.0	5		Acetone	6.7	5
	Diethylether	6.1	10		Methanol	7.4	10
	Isopentane	6.0			Water	7.4	
	Acetone	6.6			Acetone	7.1	
	Methanol	6.7			<i>n</i> -Butane	6.0	
	Water	6.2			Butene	6.2	
	<i>n</i> -Pentane	6.1			Isobutene	6.1	
	Diethylether	6.2			Dimethylether	6.3	
	Isopentane	6.2			Ammonia	6.7	
	Acetone	6.7			Methanol	8.0	
	Neopentane	6.1			Ethanol	6.4	
	R245fa	6.2	Water		8.0		
	<i>n</i> -Butane	6.6	Acetone		7.0	20	
	Butene	6.7	R245fa		6.0		
	Isobutene	6.6	<i>n</i> -Butane		6.5		
	Isobutane	6.4	Butene		6.9		
	Dimethylether	6.6	Isobutene		6.8		
	R152a	6.1	Isobutane		6.4		
	Ammonia	6.2	Dimethylether		7.8		
Methanol	7.1	R152a	7.3				
R245fa	6.0	R1234yf	6.0				
<i>n</i> -Butane	6.7	R134a	6.5				
Butene	7.1	Propane	6.5				
Isobutene	7.0	R161	7.4				
Isobutane	6.8	Ammonia	9.1				
Dimethylether	7.9	Propylene	6.6				
R152a	7.4	R32	7.3				
R1234yf	6.4	Methanol	8.1				
R134a	6.8	Ethanol	6.5				
Propane	7.0	Water	8.2				
R161	7.6	<i>n</i> -Butane	6.1	50			
Ammonia	8.4	Butene	6.7				
Propylene	7.0	Isobutene	6.6				
R32	7.2	Isobutane	6.2				
Methanol	6.7	Dimethylether	8.5				
Dimethylether	7.5	R152a	8.2				
R152a	7.2	R1234yf	6.6				
R134a	6.7	R134a	7.3				
Propane	7.2	Propane	7.6				
R161	8.2	R161	8.8				
Ammonia	10.1	Ammonia	11.5				
Propylene	7.7	Propylene	8.1				
R32	9.3	R32	10.0				
		Methanol	7.6				
		Water	7.8				

5. Conclusion

The main objective of this study is to provide a database for suitable working fluids for Worthington-type and Bush-type isobaric engines based on their performance for a wide range of low heat source temperatures and a wide range of operating pressures. To achieve this objective, a large number of potential working fluids are studied and analyzed in a systematic fashion. A novel application is introduced in this work, which is the combining of these isobaric thermomechanical engines with VCR systems. Thermodynamics models of Worthington-type and Bush-type engines are developed and simulated to study the effects of different operating temperatures and pressures on the efficiency and BWR of both engine types for 36 preselected working fluids. Results are obtained for low cycle temperature $T_C = 30^\circ\text{C}$, high cycle temperature T_H range from 40 to 300°C , and for the ΔP range from 1.0 to 100 bar. The findings and conclusions are summarized as follows: 1) A database of 36 working fluids suitable for both isobaric engines is provided for the T_H range from 40 to 300°C and for the ΔP range from 1.0 to 100 bar. 2) For the T_H range from 40 to 60°C , the achieved efficiency is very low (less than 4%) in most cases, which significantly limits practical applications in this T_H limit. 3) Ammonia and R32 have the highest efficiencies at high ΔP of 50 bar for the T_H range 100– 300°C . R161 has high performance for ΔP higher than 10 bar up to $\Delta P = 50$ bar for the full range of T_H from 80 to 300°C , which makes R161 the choice fluid for a wide range of applications. 4) For category I ($T_H = 80^\circ\text{C}$), the best performer is ammonia at $\Delta P = 20$ bar, followed by R161 at the same $\Delta P = 20$ bar, dimethyl ether at $\Delta P = 10$ bar, and *n*-butane at $\Delta P = 5$ bar, respectively. For category II ($T_H = 100^\circ\text{C}$), category III ($T_H = 140^\circ\text{C}$), and category IV ($T_H = 180^\circ\text{C}$), the best performers are ammonia, dimethyl ether, and R161, respectively, all at $\Delta P = 20$ bar. For category V ($T_H = 300^\circ\text{C}$), the best performers, in addition to ammonia, dimethyl ether, and R161, are methanol and water at $\Delta P = 20$ and 50 bar.

Acknowledgements

The work presented in this publication was made possible by NPRP-S grant # [115-1231-170155] from the Qatar National Research Fund (a member of the Qatar Foundation). The findings herein reflect the work, and are solely the responsibility, of the author.

Conflict of Interest

The author declares no conflict of interest.

Keywords

combined vapor compression refrigeration, databases of working fluids, isobaric expansion engines, refrigerants, thermomechanical refrigeration

Received: July 3, 2020

Revised: August 19, 2020

Published online: September 30, 2020

- [1] A. K. Sleiti, *Renewable Sustainable Energy Rev.* **2017**, *65*, 435.
- [2] E. J. Naimaster, A. K. Sleiti, *Energy Build.* **2013**, *61*, 153.
- [3] A. K. Sleiti, *Sol. Energy*, **2020**, 206, 68.
- [4] M. Shublaq, A. K. Sleiti, *Appl. Therm. Eng.*, **2020**, 175, 115418.
- [5] K. Mohammadi, J. G. McGowan, *J. Cleaner Prod.* **2019**, 206, 580.
- [6] K. Mohammadi, M. Saghaifar, J. G. McGowan, K. Powell, *J. Cleaner Prod.* **2019**, 238, 117912.
- [7] M. Ebrahimi, *J. Cleaner Prod.* **2017**, 142, 4258.
- [8] A. K. Sleiti, W. A. Al-Ammari, M. Al-Khawaja, *Int. J. Energy Res.* **2020**, 2020, 1.
- [9] K. Bataineh, Y. Taamneh, *Energy Build.* **2016**, 128, 22.
- [10] Z. Y. Xu, R. Z. Wang, *Sol. Energy* **2018**, 172, 14.
- [11] Q. Pan, J. Peng, H. Wang, H. Sun, R. Wang, *Sol. Energy* **2019**, 185, 64.
- [12] M. Zeyghami, D. Y. Goswami, E. Stefanakos, *Renewable Sustainable Energy Rev.* **2015**, 51, 1428.
- [13] I. Sarbu, C. Sebarchievici, *Energy Build.* **2013**, 67, 286.
- [14] K. Rahbar, S. Mahmoud, R. K. Al-Dadah, N. Moazami, S. A. Mirhadizadeh, *Energy Convers. Manage.* **2017**, 134, 135.
- [15] Z. Wu, Y. Zhang, N. Deng, *Int. J. Energy Res.* **2019**, 43, 8608.
- [16] C. Song, X. Liu, Z. Ye, M. He, *Int. J. Energy Res.* **2020**, 44, 4703.
- [17] M. Glushenkov, M. Sprenkeler, A. Kronberg, V. Kirillov, *Appl. Energy* **2012**, 97, 743.
- [18] F. Ahmed, H. Huang, S. Ahmed, X. Wang, *Int. J. Energy Res.* **2019**, 44, 6098.
- [19] A. Touré, P. Stouffs, *Energy* **2014**, 76, 445.
- [20] Y. M. Kim, D. K. K. Shin, J. H. H. Lee, in *Int. Refrigeration and Air Conditioning Conf.* **2004**, <http://docs.lib.purdue.edu/iracc/719>.
- [21] B. Nesbitt, *Handbook of Pumps and Pumping*, Elsevier Science & Technology Books **2006**.
- [22] V. Bush, *Environ. Int.* **1996**, 20, 6.
- [23] A. K. Sleiti, A. Rasras, W. Jafar, M. Alam, M. Glushenkov, A. Kronberg, in *ICTEA Int. Conf. Thermal Engineering*, Ryerson University Library, Canada **2018**, 2018, pp. 4–8.
- [24] M. Glushenkov, A. Kronberg, T. Knoke, E. Y. Kenig, *Energies* **2018**, 11, 154.
- [25] S. Aphornratana, T. Sriveerakul, *Energy Convers. Manage.* **2010**, 51, 2557.
- [26] D. Luo, A. Mahmoud, F. Cogswell, *Energy* **2015**, 85, 481.
- [27] D. Setiawan, I. D. M. Subrata, Y. A. Purwanto, A. H. Tambunan, *IOP Conf. Ser. Earth Environ. Sci.* **2018**, 147, 012035.
- [28] R. Rayegan, Y. X. Tao, *Renewable Energy* **2011**, 36, 659.
- [29] J. Kajurek, A. Rusowicz, A. Grzebielec, W. Bujalski, K. Futyma, Z. Rudowicz, *Energy* **2019**, 168, 1.
- [30] T. C. Hung, *Energy Convers. Manage.* **2001**, 42, 539.
- [31] M. A. Emadi, N. Chitgar, O. A. Oyewunmi, C. N. Markides, *Appl. Energy* **2020**, 261, 114384.
- [32] J. Bao, L. Zhang, C. Song, N. Zhang, X. Zhang, G. He, *Sustainable Energy Technol. Assessments* **2020**, 37, 100595.
- [33] J. Bao, L. Zhao, *Renewable Sustainable Energy Rev.* **2013**, 24, 325.
- [34] S. D. Wayne, C. Turner, *Energy Management Handbook*, Fairmont Press, Inc., Lilburn, GA **2006**.
- [35] U.S. Energy Information Administration, <https://www.eia.gov/totalenergy/data/annual/> (accessed: June 2020).
- [36] ASME, *Worthington Direct-Acting Simplex Steam Pump from the USS Monitor*, USS Monitor Center, Newport News, VA **2016**
- [37] V. Bush, US2157229 **1939**.
- [38] K. Wang, S. R. Sanders, S. Dubey, F. H. Choo, F. Duan, *Renewable Sustainable Energy Rev.* **2016**, 62, 89.
- [39] M. Bianchi, A. De Pascale, *Appl. Energy* **2011**, 88, 1500.
- [40] G. P. Hammond, J. B. Norman, *Appl. Energy* **2014**, 116, 387.
- [41] F. Heberle, D. Brüggemann, *Energies* **2015**, 8, 2097.
- [42] R. Li, H. Wang, Q. Tu, *Energy Technol.* **2018**, 6, 1011.
- [43] H. Chen, D. Y. Goswami, E. K. Stefanakos, *Renewable Sustainable Energy Rev.* **2010**, 14, 3059.
- [44] T. Knoke, E. Y. Kenig, A. Kronberg, M. Glushenkov, *Chem. Eng. Trans.* **2017**, 57, 499.